UvA-DARE (Digital Academic Repository)

Supramolecular bulky phosphines comprising 1,3,5-triaza-7-phosphaadamantane and Zn(salphen)s: structural features and application in hydrosilylation catalysis

Anselmo, D.; Gramage-Doria, R.; Besset, T.; Escárcega-Bobadilla, M.V.; Salassa, G.; Escudero-Adán, E.C.; Belmonte, M.M.; Martin, E.; Reek, J.N.H.; Kleij, A.W.

Link to publication

PAPER

Supramolecular bulky phosphines comprising 1,3,5-triaza-7-phosphaadamantane and Zn(salphen)s: structural features and application in hydrosilylation catalysis†

Daniele Anselmo,[a] Rafael Gramage-Doria,[b] Tatiana Besset,[b]
Martha V. Escárcega-Bobadilla,[a] Giovanni Salassa,[a] Eduardo C. Escudero-Adán,[a]
Marta Martínez Belmonte,[a] Eddy Martin,[a] Joost N. H. Reek*[b] and Arjan W. Kleij*[a,c]

The use of the commercially available, bifunctional phosphine 1,3,5-triaza-7-phosphaadamantane (abbreviated as PN_3) in conjunction with a series of Zn(salphen) complexes leads to sterically encumbered phosphine ligands as a result of (reversible) coordinative Zn–N interactions. The solid state and solution phase behaviour of these supramolecular ligand systems have been investigated in detail and revealed their stoichiometries in the solid state observed by X-ray crystallography, and those determined in solution by NMR and UV-Vis spectroscopy. Also, upon application of these supramolecular bulky phosphines in hydrosilylation catalysis employing 1-hexene as a substrate, the catalysis data infer the presence of an active Rh species with two coordinated, bulky PN_3/Zn(salphen) assembly units having a maximum of three Zn(salphen)s associated per PN_3 scaffold, with an excess of bulky phosphines hardly affecting the overall activity.

Introduction

Supramolecular catalysis has witnessed the development of a wide variety of catalyst structures showing unprecedented activity, selectivity and/or stability behaviour.[1] The common feature in all these catalysts is that the individual components self-assemble into the desired structures with high efficiency and little synthetic effort, which is highly attractive in cases where modular changes are (or tend) to be rapidly evaluated through the use of large libraries of ligands.[2] Structural diversity and accessibility are important parameters for the individual building blocks of a supramolecular catalyst. In this respect, we and others have reported on the use of various supramolecular strategies that involve Schiff base derived chiral diols,[3] phosphine-based pyridones,[4] porphyrin,[5] salen[6]

and other types of modular synthons[7] useful for catalyst optimization.

Previously, we reported on the use of bis- and tris-(pyridyl)-phosphines and their coordination chemistry towards various Lewis acidic Zn-based building blocks providing partially encapsulated supramolecular phosphines that show unusual reactivity and/or selectivity behaviour in hydroformylation catalysis.[5,6,8] The key factor adding to the success of this coordination chemistry driven strategy is the selective nature of formation of the Zn–N motifs, thereby leaving the phosphine donor available for coordination to transition metal ions and subsequent catalytic applications. Thus, these pyridylphosphines may be regarded as bifunctional ligands able to coordinate to a combination of (both) main group and transition metal ions. A minor drawback of the pyridylphosphine scaffold is that variations of the ligand backbone are limited. In order to be able to further increase the potential of the encapsulation strategy, other bifunctional *P,N*-derived scaffolds would be interesting to be considered.

Despite the fact that 1,3,5-triaza-7-phosphaadamantane is a commercially available compound and its use as a phosphine ligand in homogeneous catalysis is well-documented (Scheme 1),[9] no prior use of this "PN_3" ligand scaffold has been reported to date in the context of supramolecular catalysis. In view of the closer mutual distance between the P- and N-donor atoms of this system and the objective to access an encapsulated phosphine ligand that can potentially show markedly different

[a]*Institute of Chemical Research of Catalonia (ICIQ), Av. Països Catalans 16, 43007 – Tarragona, Spain. E-mail: akleij@iciq.es; Fax: +34 977920224; Tel: +34 977920247*
[b]*Homogeneous and Supramolecular Catalysis, Van't Hoff Institute for Molecular Sciences, University of Amsterdam, Postbox 94720, 1090 GS Amsterdam, The Netherlands. E-mail: J.N.H.Reek@uva.nl; Fax: +31-20-5255604*
[c]*Catalan Institute for Research and Advanced Studies (ICREA), Pg. Lluís Companys 23, 08010 Barcelona, Spain*
†Electronic supplementary information (ESI) available: Further experimental data, copies of relevant MS and NMR spectra of known and new compounds, and crystallographic details. CCDC 893436–893441. For ESI and crystallographic data in CIF or other electronic format see DOI: 10.1039/c3dt00078h
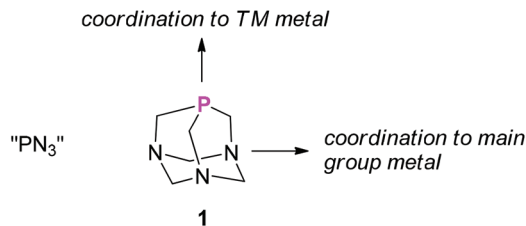
Scheme 1 Structure of the "PN$_3$" ligand scaffold **1** used in this work. TM stands for transition metal.
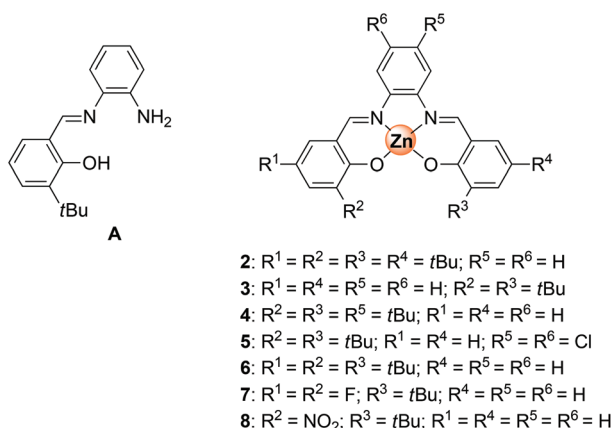
catalytic behaviour compared with the non-encapsulated ligand, we envisioned that combination with Zn(salphen) complexes (salphen = *N,N'*-bis(salicylidene)imine-1,2-phenylenediamine] would give high probability in this perspective. These Zn(salphen) complexes are readily available, modular building blocks[10] that allow for easy fine-tuning of the supramolecular assemblies, and thus their catalytic performance.[6]

Herein we report a detailed study on the assembly formation of the PN$_3$ ligand scaffold (Scheme 1) and a series of Zn(salphen)s with different substitution patterns, both in solution phase as well as in the solid state. The results from various Job plot analyses, UV–Vis titrations and application of these supramolecular PN$_3$ assemblies in hydrosilylation catalysis show that the steric properties of these encumbered ligands can be used for catalyst reactivity control.

Results and discussion

Synthesis

Whereas **4** (yield: 68%) was prepared using 4-*tert*-butyl-1,2-phenylenediamine, 3-*tert*-butylsalicylaldehyde and Zn(OAc)$_2$·2H$_2$O in a one-pot approach, non-symmetrically substituted complexes **7** (yield: 89%) and **8** (yield: 70%) were derived from the reaction of mono-imine **A** (Scheme 2)[11] and 3,5-di-fluorosalicylaldehyde and 3-nitro-salicylaldehyde, respectively, in the presence of Zn(OAc)$_2$·2H$_2$O. All other Zn(salphen) complexes (**2**, **3**, **5** and **6**) have been reported previously (see the Experimental section).[12,13]

2: R^1 = R^2 = R^3 = R^4 = *t*Bu; R^5 = R^6 = H
3: R^1 = R^4 = R^5 = R^6 = H; R^2 = R^3 = *t*Bu
4: R^2 = R^3 = R^5 = *t*Bu; R^1 = R^4 = R^6 = H
5: R^2 = R^3 = *t*Bu; R^1 = R^4 = H; R^5 = R^6 = Cl
6: R^1 = R^2 = R^3 = *t*Bu; R^4 = R^5 = R^6 = H
7: R^1 = R^2 = F; R^3 = *t*Bu; R^4 = R^5 = R^6 = H
**8**: R^2 = NO$_2$; R^3 = *t*Bu; R^1 = R^4 = R^5 = R^6 = H

Scheme 2 Line drawings of Zn(salphen) complexes **2–8** and mono-imine **A**.

NMR studies

First, a series of various Zn(salphen)s (Scheme 1) were combined in solution ([d$_6$]acetone) with the PN$_3$ ligand to investigate the binding properties. As a representative case, increasing amounts of complex **2** were added to the PN$_3$ ligand **1** with stoichiometries ranging from 1 : 1 to 3 : 1, and their ^{1}H and ^{31}P{^{1}H} NMR spectra were recorded. The results were compared with the individual components (*i.e.*, "free" PN$_3$ **1** and **2**) and clearly showed features of a binding event (ESI†). For instance, while the free phosphine PN$_3$ **1** shows a resonance at −99.0 ppm, the 1 : 1 (δ = −95.3 ppm), 2 : 1 (δ = −92.8 ppm) and 3 : 1 (δ = −92.5 ppm) combinations of **2** and PN$_3$ **1** show distinct values. It is important to notice that the addition of a third equivalent of **2** does not significantly change the ^{31}P chemical shift observed with a 2 : 1 ratio, which clearly suggests the weak influence of a possible third Zn(salphen) binding on the phosphorus nuclei. Similar features were noted in the ^{1}H NMR spectra recorded for these combinations, and a typical upfield shift was observed for the imine-H of **2** ($\Delta\delta$ = −0.38) for the 2 : 1 stoichiometry. Interestingly, further addition of **2** to **1** (*i.e.*, having a 3 : 1 ratio) led the imine-H to a downfield shifted value from 8.73 to 8.82 ppm, suggesting the presence of free, unbound **2** and observation of an average value for the imine-H resonances of the 2 : 1 assembly and free **2**. To gain more insight into the molecular structures, a series of crystallographic analyses were performed for assemblies based on **1** and various Zn(salphen)s (*vide infra*).

X-ray diffraction studies

Suitable crystals were obtained from either hot solutions in CH$_3$CN, from CH$_3$CN/DCM or from acetone (see the Experimental section). The molecular structures for the assemblies based on **1** and complexes **2** and **7** are presented in Fig. 1 and 2. The structures for **1**·(**3**)$_3$, **1**·(**4**)$_2$, **1**·(**5**)$_2$, **1**·(**6**)$_2$ and **1**·(**8**)$_2$ were also determined and these are provided in the ESI† as they are
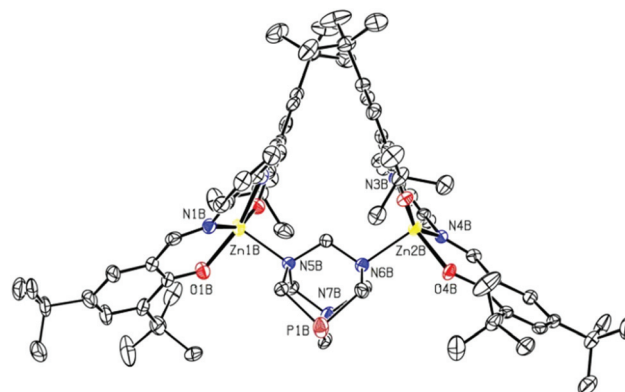
Fig. 1 Molecular structure for **1**·(**2**)$_2$ with a partial numbering scheme provided. H-atoms and co-crystallized solvent molecules are not shown for clarity reasons. Selected bond lengths (Å) and angles (°) with esd's in parentheses: Zn(1B)–O(1B) = 1.976(3), Zn(1B)–O(2B) = 1.967(3), Zn(1B)–N(1B) = 2.091(4), Zn(1B)–N(2B) = 2.099(4), Zn(1B)–N(5B) = 2.103(6), Zn(2B)–N(6B) = 2.172(7); O(1B)–Zn(1B)–O(2B) = 102.58(13), N(1B)–Zn(1B)–N(2B) = 77.31(15), O(1B)–Zn(1B)–N(2B) = 162.78(14), O(2B)–Zn(1B)–N(1B) = 156.30(14).
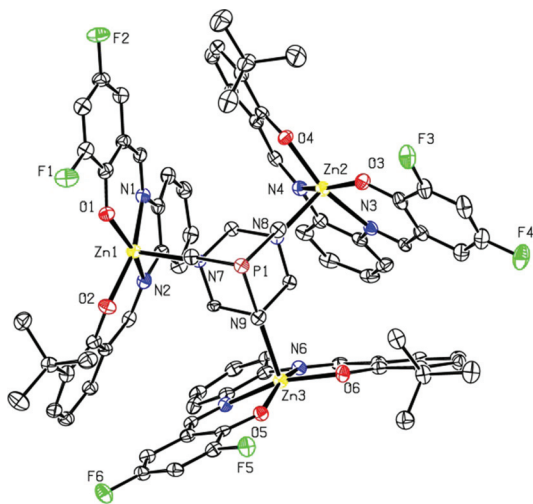
Fig. 2 Molecular structure for **1**·(**7**)$_3$ with a partial numbering scheme provided. H-atoms and co-crystallized solvent molecules are not shown for clarity reasons. Selected bond lengths (Å) and angles (°) with esd's in parentheses: Zn(1–O(1) = 1.957(3), Zn(1)–O(2) = 1.976(3), Zn(1)–N(1) = 2.107(4), Zn(1)–N(2) = 2.071(4), Zn(1)–N(7) = 2.194(4), Zn(2)–N(8) = 2.201(4), Zn(3)–N(9) = 2.200(3); O(1)–Zn(1)–O(2) = 95.68(14), N(1)–Zn(1)–N(2) = 78.93(15), O(1)–Zn(1)–N(2) = 159.16(14), O(2)–Zn(1)–N(1) = 157.88(14).

rather similar to those reported in Fig. 1 and 2. These structures confirm the preferred coordination of the N-atoms to the Zn centres in the Zn(salphen) complexes. In the case of complexes **2**, **4**, **5** and **6**, 2:1 coordination complexes were formed whereas for Zn(salphen)s **3** and **7**, 3:1 stoichiometries are present in the solid state. Upon comparing the structures in Fig. 1 and 2, being representative examples of 2:1 and 3:1 assemblies, some differences can be noted for the Zn(salphen) complexes bound to PN$_3$ **1**. First, the Zn–N(PN$_3$) bond lengths in the 2:1 assembly **1**·(**2**)$_2$ are slightly shorter on average (2.103(6) and 2.172(7) Å) compared with those observed within **1**·(**7**)$_3$ (2.194(4), 2.201(4) and 2.200(3) Å). Also, a clear difference for the O–Zn–O angle in the Zn(salphen) units is apparent in both assemblies: whereas in **1**·(**2**)$_2$ this angle is 102.58(13)°, in **1**·(**7**)$_3$ the value is much smaller (95.68(14)°). Such differences could be the result of some unfavourable steric impediment between the salphen units in the latter assembly, leading to a higher distortion from the standard encountered square pyramidal geometry around these Zn(salphen) structures.[14] Notably, the Zn(salphen) units in **1**·(**7**)$_3$ are arranged such that the different substituents (F and *t*Bu groups) of the individual complexes are pointing towards each other so as to minimize this steric penalty.

Stoichiometry in solution and titration studies

Next, we examined the stoichiometry of all assemblies in solution using ^{1}H NMR Job plot analyses and UV-Vis titration data. The results of these studies have been combined with those obtained in the solid state, and are listed in Table 1. A representative Job plot (for assembly **1**·(**2**)$_2$) is shown in Fig. 3. For all Zn(salphen)s used we found that the preferred

Table 1 Zn(salphen) complexes **2**–**8** used in this work and the stoichiometries of the PN$_3$ assemblies. S.S. = solid state stoichiometry, Sol = solution phase stoichiometry. See Scheme 1 for structural details. [Zn] stands for the Zn(salphen) complex used

[Zn]	R^1	R^2	R^3	R^4	R^5	R^6	S.S.[a]	Sol.[b]
2	*t*Bu	*t*Bu	*t*Bu	*t*Bu	H	H	2:1	2:1
3	H	*t*Bu	*t*Bu	H	H	H	3:1	2:1[c]
4	H	*t*Bu	*t*Bu	H	*t*Bu	H	2:1	2:1[c]
5	H	*t*Bu	*t*Bu	H	Cl	Cl	2:1	2:1[c]
6	*t*Bu	*t*Bu	*t*Bu	H	H	H	2:1	2:1
7	F	F	*t*Bu	H	H	H	3:1	2:1
8	H	NO$_2$	*t*Bu	H	H	H	2:1	2:1

[a] Obtained by X-ray diffraction studies. [b] Obtained *via* Job plot analyses using ^{1}H NMR in [d$_6$]acetone at 25 °C. [c] Extrapolated value from a UV-Vis titration experiment in pre-dried toluene (see ESI for more details).

stoichiometry upon combination with PN$_3$ **1** is 2:1, which is a bit unexpected if the 3:1 stoichiometries for **1**·(**3**)$_2$ and **1**·(**7**)$_2$ are considered. We therefore investigated the binding of several of these Zn(salphen) complexes by UV-Vis titrations carried out in toluene.

First of all, to get insight into the strength of the Zn–N interaction, we used Zn(salphen) complex **2** and titrated a solution thereof in toluene with PN$_3$ **1** (see also ESI†). The titration curve at λ = 438 nm and the corresponding data fit using Specfit/32[15] software are presented in Fig. 4. The model used for data-fitting considers four coloured species namely **2** and the 1:1, 2:1 and 3:1 assemblies. Specfit/32 was used to simulate both the UV-Vis traces for all these species as well as their concentration profiles (see ESI†). From the data fit the stepwise constants $K_{1:1}$, $K_{1:1\rightarrow2:1}$, and $K_{2:1\rightarrow3:1}$ were calculated as well as the cooperativity factors. As may be expected both $K_{1:1}$ (8.45 × 10^5 M^{-1}) as well as $K_{1:1\rightarrow2:1}$ (8.85 × 10^5 M^{-1}) are quite similar with negligible cooperativity (α = 1.05), while the binding of a third Zn(salphen) complex to PN$_3$ **1** ($K_{2:1\rightarrow3:1}$ = 7.51 × 10^3 M^{-1}; α = 0.05) is shown to be much weaker probably as a result of steric infringement.

Highly similar titration curves were obtained for assemblies **1**·(**n**)$_2$ (**n** = 3, 4 or 5) (see ESI†); thus it seems reasonable to assume that also in these cases the 2:1 stoichiometry is preferred in solution as indicated in Table 1. It also suggests that the binding of a third Zn(salphen) complex to **1** is comparatively weak in solution, whereas in the solid state stabilization of 3:1 stoichiometries (*i.e.*, in the case of **3** and **7**) through intermolecular interactions/packing effects may be important for the formation of 3:1 species.

As a final control experiment, the use of a generally more strongly binding Ru(CO)(salphen) complex **9** (Fig. 5)[14b,16] with a similar molecular size was probed in the presence of PN$_3$ **1** to see whether this would lead to higher stability of a possible 3:1 stoichiometry in solution. The combination of three equivalents of complex **9** with one equivalent of PN$_3$ in [d$_6$]-acetone solution resulted in a mixture of several compounds as deduced from the ^{1}H NMR spectrum (see ESI†), and the ^{31}P{^{1}H} NMR showed two signals at δ = −31.1 and −48.9 ppm.
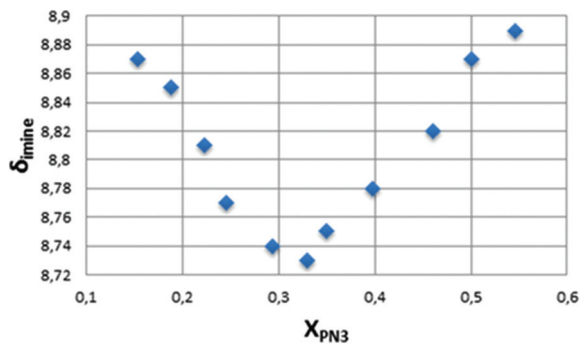
Fig. 3 Job plot analysis (^{1}H NMR, [d$_6$]acetone) using PN$_3$ **1** and Zn(salphen) complex **2**.

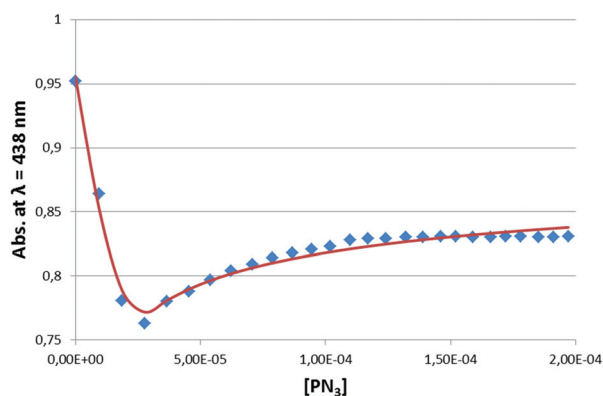**Fig. 4** Titration data (blue squares) at $\lambda = 438$ nm for the addition of PN$_3$ **1** to complex **2** in toluene (**2** at 5.38×10^{-5} M); in red the corresponding data fit.
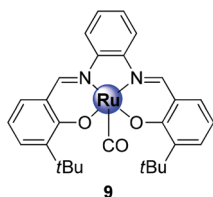

Fig. 5 Line drawing of the Ru(salphen) complex **9**.

These results sharply contrast the findings of tris-pyridylphosphine binding at Ru(salphen)s, where only one single peak in the NMR spectrum was observed.[14b] Detailed inspection of the NMR spectra revealed that beside the presence of assembled species also "free" Ru(salphen) **9** was present demonstrating that exclusive 3 : 1 stoichiometries in solution phase can also not be obtained using a more strongly binding complex. Furthermore, the ^{31}P{^{1}H} NMR also showed that the binding process is not selective, as clear indications of Ru–P coordination were apparent from ^{31}P resonances found in the region −50 to −30 ppm (ESI†).[9] The occurrence of Ru-to-P coordination can be tentatively explained by the fact that the PN$_3$ ligand **1** is a much more basic phosphine than previously used tris-pyridylphosphines.[17] Addition of 20% v/v of a competing ligand (*i.e.*, [d$_5$]pyridine) furnished both the ^{1}H and ^{31}P{^{1}H}

traces more easy to interpret, and confirmed the initial and only partial P-coordination mode of the PN$_3$ ligand **1** (ESI†).

Catalysis studies

In order to evaluate the supramolecular phosphines in catalysis, first hydroformylation reactions were carried out using styrene, 1-octene and *trans*-2-octene as substrates as the aldehyde product selectivity has shown to be a function of the steric and electronic properties of the phosphine ligand. The results gathered in these first studies are reported in Tables S1–S3 (ESI†). The use of PN$_3$ **1** and various Zn(salphen) complexes (**2**–**4**) combined with [Rh(acac)(CO)$_2$] (acac = acetylacetonate) to form complexes coordinated by bulky phosphine ligands that can stir catalyst activity and/or product selectivity gave poor results and in general with the three substrates tested only small changes in product selectivity were noted; only in the case of *trans*-2-octene some increase in product selectivity (C3 : C2 aldehyde ratio = 51 : 49) was observed reminiscent of previous results reported by part of us using a porphyrin-derived supramolecular phosphoroamidite ligand.[18] Further to this, preliminary investigations on palladium-based allylic alkylation (ESI, Table S4†) revealed that the supramolecular ligands PN$_3$/Zn(salphen) slightly increased the branched product formation by about 10% compared to the background reaction (*i.e.*, the use of PN$_3$ **1** only), suggesting some degree of steric regulation.

Therefore, we decided to apply the supramolecular bulky phosphines in another reaction, and hydrosilylation (Scheme 3) was then chosen to evaluate the influence of the steric bulk of the PN$_3$/Zn(salphen) ligand assemblies given the precedent provided by the work of Tsuji and coworkers.[19] It should be noted that Tsuji used covalent bulky phosphines, for which the steric influence was evaluated in terms of activity, and particularly when using an excess of phosphine ligand. The more sterically demanding phosphines did not allow for more than two P-ligands to be simultaneously coordinated to the Rh metal centre and thus catalytic activity was preserved unlike noted for less bulky phosphines such as PPh$_3$. This hydrosilylation protocol may serve as a tool to assess whether the supramolecular phosphines based on PN$_3$ **1** and Zn(salphen)s show similar sterically controlled reactivity
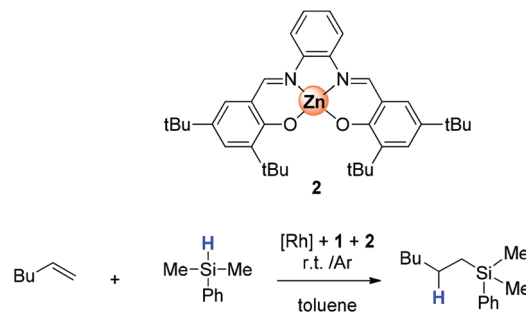
Scheme 3 Hydrosilylation catalysis carried out with the supramolecular bulky phosphine based on PN$_3$ **1** and Zn(salphen) complex **2**. [Rh] stands for the rhodium precursor [Rh-μ-Cl(C$_2$H$_4$)$_2$]$_2$.

Table 2 Hydrosilylation of 1-hexene using dimethylphenylsilane and phosphine ligands derived from PN3 **1** and Zn(salphen) **2**[a]

Entry	[P]	Equiv. [P]	Equiv.[b] [Zn]	Conv.[c] (%)	Yield[c] (%)
1	PPh₃	2	0	100	98
2	PPh₃	4	0	0	0
3	**1**	2	0	83	82
4	**1**	4	0	0	0
5	**1**	2	2	52	51
6	**1**	2	4	30[d]	29[d]
7	**1**	2	6	79	76
8	**1**	2	8	43[e]	42[e]
9	**1**	4	4	0	0
10	**1**	4	8	27	25
11	**1**	4	12	74[d]	73[d]
12	**1**	4	16	0[e]	0[e]
13[f]	—	—	2	0	0

[a] Reaction conditions: 1-hexene (1.0 mmol), silane (1.2 mmol), [Rh-μ-Cl(C₂H₄)₂]₂ (5 μmol), toluene (1.0 mL), r.t., Ar-atmosphere, 1 h. [b] [Zn] = Zn(salphen) complex **2**. [c] Conversion/yield determined by ¹H NMR; yield determined using mesitylene as an internal standard. [d] Average of two runs with both runs within 1–2%. [e] Heterogeneous mixture observed. [f] Reaction without the Rh precursor present.

and thus can give synthetically more easily accessible alternative bulky P-ligands. 1-Hexene and dimethylphenylsilane were selected as reaction partners and the catalytic reactions were performed in toluene at room temperature for 1 h (Table 2). The results were compared to those obtained for a typical phosphine ligand (PPh₃) using various phosphine-to-metal stoichiometries.

The presence of two equiv. of PPh₃ is known to produce an active catalyst,[19] and an excess of PPh₃ (entry 2, Table 2) shuts down catalytic turnover completely. The same trend is noted for PN₃ **1** (entries 3 and 4). Then, the influence of an increasing amount of Zn(salphen) **2** (entries 5–7) was evaluated first using two equiv. of PN₃ **1** with respect to the Rh precursor. In the presence of one equiv. (on average) of Zn(salphen) per phosphine, a much higher conversion level (52%) and yield of the product was observed (51%) and further addition of two equiv. of Zn(salphen) **2** caused some decrease in activity, which we ascribe to a steric effect that results in a less efficient activation of the silylating agent by the Rh complex. When 3 equiv. of Zn(salphen) per PN₃ **1** are present (entry 7) the intermediate may be more prone to phosphine dissociation giving, on an average, a more active system. Thus, in the presence of six equiv. of Zn(salphen) complex (entry 7) the PN₃ ligands likely become saturated with Zn(salphen)s through N→Zn coordination but the original activity (entry 1) is nearly fully recovered (79% conversion; yield 76%) as a result of an increasing steric impediment posed by the coordinated, bulky PN₃/Zn(salphen) ligand assemblies.

In the work of Tsuji,[19] covalent bulky phosphines still provided high activity catalyst systems even when an excess (4 equiv.) of the phosphine was present. Therefore, we also tested the activity of the catalyst prepared in situ using 4 equiv. of PN₃ **1** and 4–12 equiv. of Zn(salphen) **2** (entries 9–11, Table 2). The highest conversion/yield was again noted when 3 equiv. (on average) of Zn complex per PN₃ ligand **1** were used (entry 11)

and the yield was close to the one reported when only two equiv. of the supramolecular phosphine were combined with the Rh precursor. The presence of an excess of Zn(salphen) (i.e., 4 equiv. per PN₃ **1**) either using a total of two equiv. or four equiv. of PN₃ **1** per Rh precursor (entries 8 and 12) did not lead to higher conversions/yields; in contrast, a much less efficient system was obtained and the heterogeneous character (red solid formation) of the reaction mixture in these cases is likely the principal reason for this observation. Apparently, upon using an excess of Zn(salphen) **2** (part of) the (pre)catalytic species precipitates.

Following the observations from Tsuji,[19] the most likely precursor catalyst to be formed in the presence of two equiv. of phosphine is a trans-bis-phosphine Rh complex having an additional chloride and alkene coordinating. While an increase in the relative amount of Zn(salphen) versus PN₃ **1** first leads to a decrease in activity (Table 2, entry 5 → entry 6), further saturation of the PN₃ scaffold with the Zn complex **2** may give rise to a more dynamic inter-conversion between four- and three-coordinated Rh species thus creating vacant coordination sites for catalytic turnover and thus higher activity. The latter situation was also studied by ³¹P{¹H} NMR (Fig. 6c) and compared with the free PN₃/Zn(salphen) assembly (Fig. 6b, $\delta = -92.5$ ppm) and showed the presence of a single complex (see the inset of Fig. 6c; $\delta = -47.2$ ppm) with a characteristic $^1J_{(P-Rh)} = 131$ Hz close to the trans-diphosphine complexes Rh complexes derived from either the bulky P-ligand communicated by Tsuji ($^1J_{(P-Rh)} = 130$ Hz)[19] or PPh₃ ($^1J_{(P-Rh)} = 129$ Hz).[20]

Since the presence of an excess of PN₃/Zn(salphen) ligand assembly (Table 2, entry 11) showed the highest reactivity, also this case was studied in more detail using ³¹P{¹H} NMR (see
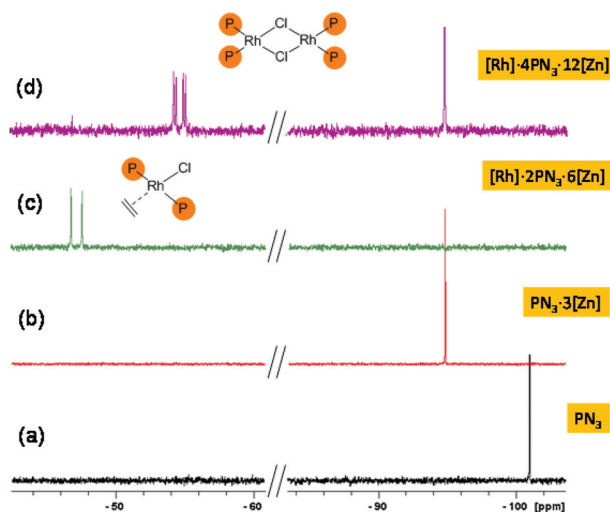
Fig. 6 NMR details of the hydrosilylation pre-catalysts using different amounts of PN₃ **1** and/or Zn(salphen) **2**. Conditions: [d₆]acetone, r.t., stirred for two hours in those cases where the Rh salt was added. (a) Only PN₃ **1** present; (b) mixture of PN₃ **1** and 3 equiv. of Zn(salphen) **2**; (c) mixture of 1 equiv. of [Rh(μ-Cl)(C₂H₄)₂]₂, 2 equiv. of PN₃ **1** and 6 equiv. of Zn(salphen) **2**; (d) mixture of 1 equiv. of [Rh(μ-Cl)(C₂H₄)₂]₂, 4 equiv. of PN₃ **1** and 12 equiv. of Zn(salphen) **2**. The graphical insets show the proposed structures.

Fig. 6D). Two species were detected, with one being easily identified as the free PN$_3$/Zn(salphen) ligand assembly (δ = −92.5 ppm) showing that not all the supramolecular phosphine interacts with the Rh metal center. The second species (δ = −54.6 ppm), a Rh-containing complex different from the one observed in the presence of only two equiv. of supramolecular ligand, pertains to a double doublet (dd, $^1J_{(P–Rh)}$ = 142 Hz; $^2J_{(P–P)}$ = 36.8 Hz). The $^2J_{(P–P)}$ coupling is typical for *cis*-diphosphine–Rh complexes,[21] and the formation of a dinuclear Rh complex (see the inset of Fig. 6D) as proposed by Tsuji for his bulky phosphine complexes is anticipated. The presence of bridging chlorides effectively prevents the formation of *trans*-bis-phosphine complexes. The presence of tris-phosphine Rh complexes can be ruled out as in that case a more complicated ^{31}P NMR would be expected. Apparently, the bulkiness of the PN$_3$/Zn(salphen) ligand assembly does not allow for the formation of (catalytically inactive) tri- or tetraphosphine species, and signal integration for both P-containing compounds present (Fig. 6D; ~1 : 1) is in good agreement with the hypothesis that only two phosphines can simultaneously coordinate to the Rh metal centre. The observed P–P coupling is probably a result of a geometrical distortion (as in the case of Tsuji's P-ligands)[19] caused by the steric impediment of the PN$_3$/Zn(salphen) ligand assembly, with both magnetically distinct P centres in fast equilibrium.

Conclusions

This work has shown that supramolecular phosphines based on the PN$_3$ scaffold are indeed easily prepared by simple combination of a series of Zn(salphen) complexes and PN$_3$ **1** in solution giving rise to assembled structures with a preferable 2 : 1 stoichiometry. The latter has been supported by various analyses (Job plot analysis, UV-Vis titrations, and control experiments). The catalytic results, and in particular those obtained using the PN$_3$/Zn(salphen) ligand assemblies in hydrosilylation, clearly show that the supramolecular formation of bulky phosphines with little synthetic effort may be useful as an alternative for covalent phosphines,[19] and the hydrosilylation catalysis data for 1-hexene have shown comparable effects between covalent and supramolecular bulky phosphine ligands. Thus, this implies that assemblies of the type PN$_3$/Zn-(salphen) may hold promise to direct catalyst reactivity and potentially process selectivity. Further catalytic studies are now underway to exploit the bulkiness of such P-ligands in other catalysed organic transformations.

Experimental section

General

NMR spectra were recorded with a Bruker AV-400 or AV-500 spectrometer and were referenced to the residual deuterated solvent signals. Elemental analysis was performed by the Unidád de Análisis Elemental at the Universidad de Santiago de Compostela. Mass spectrometric analysis and X-ray diffraction studies were performed by the Research Support Group at the ICIQ. Complexes **2**,[12] **3**,[12] **5**[12] and **6**[13] were prepared according to previously reported procedures. Mono-imine **A**[11] and Zn(TPP) **10**[22] were prepared according to known procedures.

Synthesis of Zn(salphen) (4)

A mixture of 3-*tert*-butylsalicylaldehyde (390 mg, 2.19 mmol), 4-*tert*-butyl-*ortho*-phenylenediamine (180 mg, 1.09 mmol) and Zn(OAc)$_2$·2H$_2$O (360 mg, 1.64 mmol) in MeOH (25 mL) was stirred at room temperature for 48 h. Then the product was collected by filtration to furnish a light orange product (406 mg, 68%). ^{1}H NMR (400 MHz, [d$_6$]acetone): δ = 9.14 (s, 1H, CH=N), 9.04 (s, 1H, CH=N), 7.96 (d, ^4J = 2.0 Hz, 1H, ArH), 7.83 (d, ^3J = 8.6 Hz, 1H, ArH), 7.44 (d, ^4J = 2.0 Hz, ^3J = 8.6 Hz, 1H, ArH), 7.23–7.28 (m, 4H, ArH), 6.46 (t, ^3J = 7.6 Hz, 2H, ArH), 1.52 (s, 18H, C(CH$_3$)$_3$), 1.41 (s, 9H, C(CH$_3$)$_3$); ^{13}C{^{1}H} NMR (125 MHz, [d$_6$]acetone): δ = 182.58, 162.34, 161.91, 150.12, 141.99, 139.21, 137.35, 134.23, 130.35, 124.09, 119.66, 115.17, 112.41, 49.0, 35.12, 34.79, 30.72; MS (MALDI+, DCTB): m/z = 546.1 [M]$^+$ (calcd 546.2); elemental analysis calculated for C$_{32}$H$_{38}$N$_2$O$_2$Zn·2H$_2$O: C 65.80, H 7.25, N 4.80; found: C 65.53, H 8.27, N 4.61.

Synthesis of Zn(salphen) (7)

To a solution of mono-imine **A** (73 mg, 0.27 mmol) in MeOH (15 mL) were added 3,5-difluoro-salicylaldehyde (46 mg, 0.29 mmol) and Zn(OAc)$_2$·2H$_2$O (99 mg, 0.45 mmol). The solution was left stirring for 18 hours while an orange precipitate was slowly formed. The desired compound was isolated by filtration and dried *in vacuo* to yield an orange solid (114 mg, 89%). ^{1}H NMR (500 MHz, [d$_6$]acetone): δ = 8.99 (s, 1H, CH=N), 8.92 (s, 1H, CH=N), 7.84–7.81 (m, 2H, ArH), 7.47–7.37 (m, 2H, ArH), 7.25 (d, ^4J = 1.8 Hz, ^3J = 7.4 Hz, 1H, ArH), 7.20 (d, ^4J = 1.8 Hz, ^3J = 8.0 Hz, 1H, ArH), 7.03–6.97 (m, 2H, ArH), 6.43 (t, ^3J = 7.6 Hz, 1H, ArH), 1.45 (s, 9H, C(CH$_3$)$_3$); ^{13}C{^{1}H} NMR (125 MHz, [d$_6$]acetone): δ = 172.74, 163.86, 161.76, 141.94, 140.69, 139.39, 134.76, 130.80, 128.20, 126.98, 119.67, 119.25, 116.77, 113.57, 112.58, 107.93, 48.74, 35.12 + 29.46; MS (MALDI+, DCTB): m/z = 470.1 [M]$^+$ (calcd 407.1); elemental analysis calculated for C$_{24}$H$_{20}$F$_2$N$_2$O$_2$Zn·1/3H$_2$O: C 60.33, H 4.36, N 5.86; found: C 60.36, H 4.19, N 5.81.

Synthesis of Zn(salphen) (8)

To a solution of mono-imine **A** (134 mg, 0.49 mmol) in MeOH (20 mL) were added 3-nitro-salicylaldehyde (90 mg, 0.54 mmol) and Zn(OAc)$_2$·2H$_2$O (300 mg, 1.37 mmol). The resulting solution was stirred for 18 h at room temperature. In due course, a light orange suspension was obtained, which was filtered to furnish the product as a light orange solid (164 mg, 70%). ^{1}H NMR (500 MHz, [d$_6$]acetone): δ = 9.11 (s, 1H, CH=N), 8.97 (s, 1H, CH=N), 7.88 (t, ^3J = 8.5 Hz, 2H, ArH), 7.79 (d, ^4J = 2.0 Hz, ^3J = 7.9 Hz, 1H, ArH), 7.69 (d, ^4J = 1.7 Hz, ^3J = 7.7 Hz, 1H, ArH), 7.47 (t, ^3J = 7.6 Hz, 1H, ArH), 7.40 (t, ^4J = 7.6 Hz, 1H, ArH), 7.29 (d, ^4J = 1.8 Hz, ^3J = 7.3 Hz, 1H, ArH), 7.24 (d, ^4J = 1.9 Hz, ^3J = 8.0 Hz, 1H, ArH), 6.60 (t, ^3J = 7.7 Hz,

1H, ArH), 6.47 (t, ^3J = 7.6 Hz, 1H, ArH), 1.47 (s, 9H, C(CH$_3$)$_3$); ^{13}C{^{1}H} NMR (125 MHz, [d$_6$]acetone): δ = 163.85, 162.23, 142.26, 140.72, 140.29, 139.14, 134.46, 130.96, 129.16, 128.49, 126.95, 123.35, 116.46, 112.91, 111.18, 48.93, 34.94, 29.15; MS (MALDI+, pyrene): m/z = 478.9 [M]$^+$ (calcd 479.1); elemental analysis calculated for C$_{24}$H$_{21}$N$_3$O$_4$Zn·1/2H$_2$O: C 58.85, H 4.53, N 8.58; found: C 58.66, H 4.27, N 8.63.

Synthesis of Ru(CO)(salphen) (9)

A solution of *N,N'*-bis(3-*tert*-butylsalicylidene)-1,2-phenylenediamine (459 mg, 1.07 mmol) and Ru$_3$(CO)$_{12}$ (310 mg, 0.48 mmol) in toluene (25 mL) was heated under reflux for 18 h under argon.[16] The reaction mixture was cooled to room temperature, filtered through Celite, and concentrated under reduced pressure. The resulting dark red residue was chromatographed on alumina(II) eluting first with toluene to remove an orange band, followed by CH$_2$Cl$_2$ to remove a yellow band, and then with a mixture of EtOH–acetone (5 : 95 v/v) to remove a red-pink band. The red-pink band was concentrated to dryness under vacuum affording the compound as a glassy red solid that was recrystallized from aqueous EtOH. Yield: 52 mg (9%). ^{1}H NMR (500 MHz, [d$_6$]acetone): δ = 9.31 (s, 2H, CH=N), 8.29–8.27 (m, 2H, ArH), 7.44 (d, ^4J = 1.7 Hz, ^3J = 8.1 Hz, 2H, ArH), 7.36–7.32 (m, 4H, ArH), 6.51 (t, ^3J = 7.4 Hz, 2H, Ar-H), 1.54 (s, 18H, C(CH$_3$)$_3$); ^{13}C{^{1}H} NMR (125 MHz, [d$_6$]-acetone): δ = 216.51, 156.50, 142.50, 135.26, 130.65, 126.16, 115.36, 113.16, 35.51 29.35; UV-Vis (6.12 × 10^{-5} M in toluene): λ (ε) = 306 nm (17 712), 379 nm (24 020), 480 nm (7500), 527 (shoulder, 6280); Selected IR (solid): ν = 1924 (CO) cm^{-1}; MS (MALDI+, pyrene): m/z = 528.3 [M – CO]$^+$ (calcd 528.1), 1056.5 [(M – CO)$_2$]$^+$ (calcd 1056.3); elemental analysis calculated for C$_{29}$H$_{30}$N$_2$O$_3$Ru·H$_2$O: C 60.72, H 5.62, N 4.88; found: C 60.91, H 5.82, N 4.32.

Hydrosilylation catalysis

A slightly modified literature procedure was applied:[19] in a typical experiment, under an argon atmosphere, the phosphine ligand, the Zn(salphen) complex **2** and [Rh(µ-Cl)(C$_2$H$_4$)$_2$]$_2$ were placed in a Schlenk flask and 1 mL of anhydrous, degassed solvent was added by a syringe. The mixture was then stirred at room temperature for 2 h. Then 1-hexene, mesitylene (used as an internal standard) and dimethyl-phenylsilane were added by a syringe. After 1 h the conversion and the yield were determined by ^{1}H NMR using signal integration and comparison.

Coordination studies

As a primary analysis tool ^{31}P{^{1}H} NMR was used. In a typical experiment, the phosphine ligand, Zn(salphen) complex **2** and [Rh(µ-Cl)(C$_2$H$_4$)$_2$]$_2$ were placed in a Schlenk flask and 1 mL of anhydrous, degassed toluene was added by a syringe. The mixture was stirred at room temperature for 2 h. Then an aliquot was introduced in an NMR tube equipped with a capillary containing [d$_6$]acetone and a ^{31}P NMR spectrum was recorded.

UV-Vis titrations

A typical example is as follows: aliquots between 20–520 µL of a solution of PN$_3$ **1** (9.54 × 10^{-4} M) and Zn(salphen) complex **2** (5.38 × 10^{-5} M) in dry toluene were added stepwise to 2.00 mL of a solution of the host **2** in dry toluene in a 1.00 cm quartz cuvette. After each addition, a UV-Vis spectrum was acquired. UV-Vis spectra were recorded on a Shimadzu UV-1800 spectrophotometer.

Job-plot analyses

Samples for NMR Job plot analysis were prepared by mixing weighed amounts of different Zn(salphen) complexes and PN$_3$ **1** (typically the concentration of the Zn(salphen) was 1.1–2.0 × 10^{-2} M, and concentration of PN$_3$ **1** typically in the range 3.6 × 10^{-3} to 1.3 × 10^{-2} M) in 0.7 mL of [d$_6$]acetone following analysis by ^{1}H NMR spectroscopy. The δ_{imine} (CH=N) of the metal complexes was plotted against the relative molar fraction (ξ) of PN$_3$ **1** of each sample.

X-ray diffraction studies

The measured crystals were stable under atmospheric conditions; nevertheless they were treated under inert conditions immersed in perfluoropoly-ether as a protecting oil for manipulation. Data collection: measurements were made on a Bruker-Nonius diffractometer equipped with an APPEX 2 4K CCD area detector, an FR591 rotating anode with MoKα radiation, Montel mirrors and a Kryoflex low temperature device (T = −173 °C). Full-sphere data collection was used with ω and φ scans. Programs used: data collection Apex2 V2011.3 (Bruker-Nonius 2008), data reduction Saint+Version 7.60A (Bruker AXS 2008) and absorption correction SADABS V. 2008-1 (2008). Structure solution: SHELXTL Version 6.10 (Sheldrick, 2000)[23] was used. Structure refinement: SHELXTL-97-UNIX VERSION. Structure resolution was done with SIR2011.[24]

Crystallographic details for assembly **1**·(**2**)$_2$. C$_{84}$H$_{113}$N$_{10}$O$_4$PZn$_2$, M_r = 1485.55, triclinic, $P\bar{1}$, a = 15.4322(9) Å, b = 18.2236(12) Å, c = 31.756(2) Å, α = 84.459(3)°, β = 83.048(3)°, γ = 74.347(3)°, V = 8517.2(9) Å^3, Z = 4, ρ = 1.161 mg M^{-3}, μ = 0.634 mm^{-1}, λ = 0.71073 Å, T = 100(2) K, $F(000)$ = 3176, crystal size = 0.20 × 0.20 × 0.03 mm, θ(min) = 0.65°, θ(max) = 25.07°, 90 843 reflections collected, 29 658 reflections unique (R_{int} = 0.0565), GoF = 1.048, R_1 = 0.0648 and wR_2 = 0.1650 [$I > 2\sigma(I)$], R_1 = 0.0942 and wR_2 = 0.1772 (all indices), min/max residual density = −1.053/1.334 [e Å^{-3}]. Completeness to θ(25.07°) = 98.0%. The structure has been deposited at the CCDC with reference number 893436. This structure was solved using a disorder model for the *t*Bu groups of the complex and for the PN$_3$ part of one of the crystallographic independent molecules. There are six acetonitrile co-crystallized solvent molecules present in the asymmetric unit, three of them were modelled with disorder and the program Squeeze[25] was applied.

Crystal data for assembly **1**·(**3**)$_3$. C$_{181}$H$_{206}$N$_{18}$Cl$_2$O$_{12}$P$_2$Zn$_6$, M_r = 3350.70, monoclinic, Cc, a = 29.253(3) Å, b = 16.9817(16) Å, c = 33.515(3) Å, α = 90°, β = 100.630(3)°, γ = 90°, V = 16 363(3) Å^3, Z = 4, ρ = 1.360 mg M^{-3}, μ = 0.985 mm^{-1},

$\lambda = 0.71073$ Å, $T = 100(2)$ K, $F(000) = 7032$, crystal size = $0.20 \times 0.20 \times 0.05$ mm, $\theta(\text{min}) = 1.42°$, $\theta(\text{max}) = 26.82°$, 128 388 reflections collected, 34 428 reflections unique ($R_{\text{int}} = 0.0453$), GoF = 1.017, $R_1 = 0.0435$ and $wR_2 = 0.1002$ [$I > 2\sigma(I)$], $R_1 = 0.0571$ and $wR_2 = 0.1064$ (all indices), min/max residual density = $-0.846/1.542$ [e Å^{-3}]. Completeness to $\theta(26.82°) = 99.4\%$. The structure has been deposited at the CCDC with reference number 893439. This structure presents disorder in the various salphen units with occupancy ratios of 50 : 50 and 60 : 40. The structure is a DCM solvate.

Crystallographic details for assembly 1·(4)$_2$. C$_{76}$H$_{100}$N$_7$-O$_6$PZn$_2$, $M_r = 1369.34$, monoclinic, $P2(1)/c$, $a = 16.3497(13)$ Å, $b = 15.1014(11)$ Å, $c = 29.107(2)$ Å, $\alpha = 90°$, $\beta = 93.354(3)°$, $\gamma = 90°$, $V = 7174.3(9)$ Å^3, $Z = 4$, $\rho = 1.268$ mg M^{-3}, $\mu = 0.747$ mm^{-1}, $\lambda = 0.71073$ Å, $T = 100(2)$ K, $F(000) = 2912$, crystal size = $0.30 \times 0.10 \times 0.02$ mm, $\theta(\text{min}) = 1.52°$, $\theta(\text{max}) = 25.91°$, 71 356 reflections collected, 13 912 reflections unique ($R_{\text{int}} = 0.0846$), GoF = 1.017, $R_1 = 0.0547$ and $wR_2 = 0.1156$ [$I > 2\sigma(I)$], $R_1 = 0.0949$ and $wR_2 = 0.1313$ (all indices), min/max residual density = $-0.824/0.671$ [e Å^{-3}]. Completeness to $\theta(25.91°) = 99.6\%$. The structure has been deposited at the CCDC with reference number 893440. This structure shows disorder in both the adamantane backbone as well as in part of the *t*Bu groups; the molecule contains two co-crystallized acetone solvent molecules disordered over two positions.

Crystallographic details for assembly 1·(5)$_2$. C$_{64}$H$_{71}$Cl$_4$N$_8$-O$_4$PZn$_2$, $M_r = 1319.80$, monoclinic, $C2/c$, $a = 30.798(2)$ Å, $b = 13.5677(9)$ Å, $c = 29.886(2)$ Å, $\alpha = 90°$, $\beta = 101.815(2)°$, $\gamma = 90°$, $V = 12 223.7(14)$ Å^3, $Z = 8$, $\rho = 1.434$ mg M^{-3}, $\mu = 1.041$ mm^{-1}, $\lambda = 0.71073$ Å, $T = 100(2)$ K, $F(000) = 5488$, crystal size = $0.20 \times 0.15 \times 0.15$ mm, $\theta(\text{min}) = 1.35°$, $\theta(\text{max}) = 28.20°$, 211 665 reflections collected, 15 010 reflections unique ($R_{\text{int}} = 0.0466$), GoF = 1.060, $R_1 = 0.0310$ and $wR_2 = 0.0714$ [$I > 2\sigma(I)$], $R_1 = 0.0408$ and $wR_2 = 0.0753$ (all indices), min/max residual density = $-0.463/0.397$ [e Å^{-3}]. Completeness to $\theta(28.20°) = 99.7\%$. The structure has been deposited at the CCDC with reference number 893438. This structure is a CH$_3$CN solvate with disorder in both the adamantane structure as well as the co-crystallized CH$_3$CN molecules.

Crystal data for assembly 1·(6)$_2$. C$_{70.50}$H$_{88}$ClN$_7$O$_4$PZn$_2$, $M_r = 1294.64$, monoclinic, $P2(1)/c$, $a = 14.3779(7)$ Å, $b = 30.8290(15)$ Å, $c = 17.5123(8)$ Å, $\alpha = 90°$, $\beta = 110.964(2)°$, $\gamma = 90°$, $V = 7248.6(6)$ Å^3, $Z = 4$, $\rho = 1.186$ mg M^{-3}, $\mu = 0.769$ mm^{-1}, $\lambda = 0.71073$ Å, $T = 100(2)$ K, $F(000) = 2736$, crystal size = $0.35 \times 0.10 \times 0.10$ mm, $\theta(\text{min}) = 1.41°$, $\theta(\text{max}) = 26.80°$, 73 204 reflections collected, 15 211 reflections unique ($R_{\text{int}} = 0.0410$), GoF = 1.045, $R_1 = 0.0588$ and $wR_2 = 0.1798$ [$I > 2\sigma(I)$], $R_1 = 0.0751$ and $wR_2 = 0.1907$ (all indices), min/max residual density = $-0.437/2.016$ [e Å^{-3}]. Completeness to $\theta(26.80°) = 98.0\%$. The structure has been deposited at the CCDC with reference number 893441. This structure, a DCM solvate, was modelled using a disorder model for both the adamantane and part of the *t*Bu groups. For resolving this structure the program SQUEEZE[25] was used.

Crystal data for assembly 1·(7)$_3$. C$_{78}$H$_{72.5}$N$_9$F$_6$O$_{6.25}$PZn$_3$, $M_r = 1577.03$, monoclinic, $C2/c$, $a = 18.1552(4)$ Å, $b = 31.5457(8)$ Å,

$c = 25.2433(7)$ Å, $\alpha = 90°$, $\beta = 105.4820(10)°$, $\gamma = 90°$, $V = 13 932.7(6)$ Å^3, $Z = 8$, $\rho = 1.504$ mg M^{-3}, $\mu = 2.082$ mm^{-1}, $\lambda = 0.71073$ Å, $T = 100(2)$ K, $F(000) = 6500$, crystal size = $0.10 \times 0.10 \times 0.05$ mm, $\theta(\text{min}) = 2.80°$, $\theta(\text{max}) = 66.71°$, 15 899 reflections collected, 16 047 reflections unique ($R_{\text{int}} = 0.000$), GoF = 1.147, $R_1 = 0.0497$ and $wR_2 = 0.1436$ [$I > 2\sigma(I)$], $R_1 = 0.0531$ and $wR_2 = 0.1487$ (all indices), min/max residual density = $-0.556/0.513$ [e Å^{-3}]. Completeness to $\theta(66.71°) = 95.2\%$. The structure has been deposited at the CCDC with reference number 893437. This structure is a hemi-hydrate with the water molecules disordered over two positions. This sample was measured using Cu-radiation, and the sample turned out to be a combination of two crystals with a 71 : 29 occupancy ratio. For the absorption correction TWINABS was used.[26]

Note that the structure for assembly 1·(8)$_2$ was also determined; since it constitutes a very similar structure compared to the other 2 : 1 assemblies, it was not completely refined. A visual is provided in the ESI† and a res-file is available from the authors.

Notes and references

1 (*a*) *Supramolecular Catalysis*, ed. P. W. N. M. van Leeuwen, Wiley-VCH, Weinheim, Germany, 2008; (*b*) J. Meeuwissen and J. N. H. Reek, *Nat. Chem.*, 2010, **2**, 615; (*c*) T. S. Koblenz, J. Wassenaar and J. N. H. Reek, *Chem. Soc. Rev.*, 2008, **37**, 247; (*d*) M. J. Wiester, P. A. Ulmann and C. A. Mirkin, *Angew. Chem., Int. Ed.*, 2011, **50**, 114; (*e*) B. Breit, *Pure Appl. Chem.*, 2008, **80**, 855; (*f*) D. Fiedler, D. H. Leung, R. G. Bergman and K. N. Raymond, *Acc. Chem. Res.*, 2005, **38**, 349; (*g*) A. W. Kleij and J. N. H. Reek, *Chem.–Eur. J.*, 2006, **12**, 4218.

2 (*a*) M. T. Reetz, *Angew. Chem., Int. Ed.*, 2008, **47**, 2556; (*b*) C. Gennari and U. Piarulli, *Chem. Rev.*, 2003, **103**, 3071; (*c*) A. J. Sandee and J. N. H. Reek, *Dalton Trans.*, 2006, 3385; (*d*) M. B. Francis, T. F. Jamison and E. N. Jacobsen, *Curr. Opin. Chem. Biol.*, 1998, **2**, 422; (*e*) B. Breit, *Angew. Chem., Int. Ed.*, 2005, **44**, 6816.

3 (*a*) P. W. N. M. van Leeuwen, D. Rivillo, M. Raynal and Z. Freixa, *J. Am. Chem. Soc.*, 2011, **133**, 18562; (*b*) D. M. Rivillo, H. Gulyas, J. Benet-Buchholz,

E. C. Escudero-Adán, Z. Freixa and P. W. N. M. van Leeuwen, *Angew. Chem., Int. Ed.*, 2007, **46**, 7247.

4 (*a*) B. Breit and W. Seiche, *J. Am. Chem. Soc.*, 2003, **125**, 6608; for related aminopyridine derived P-ligands: (*b*) B. Breit and W. Seiche, *Angew. Chem., Int. Ed.*, 2005, **44**, 1640.

5 (*a*) V. F. Slagt, P. W. N. M. van Leeuwen and J. N. H. Reek, *Chem. Commun.*, 2003, 2474; (*b*) V. F. Slagt, M. Röder, P. C. J. Kamer, P. W. N. M. van Leeuwen and J. N. H. Reek, *J. Am. Chem. Soc.*, 2004, **126**, 4056; (*c*) A. M. Kluwer, R. Kapre, F. Hartl, M. Lutz, A. L. Spek, A. M. Brouwer, P. W. N. M. van Leeuwen and J. N. H. Reek, *Proc. Natl. Acad. Sci. U. S. A.*, 2009, **26**, 10460.

6 (*a*) M. Kuil, P. E. Goudriaan, P. W. N. M. van Leeuwen and J. N. H. Reek, *Chem. Commun.*, 2006, 4679; (*b*) A. W. Kleij, M. Lutz, A. L. Spek, P. W. N. M. van Leeuwen and J. N. H. Reek, *Chem. Commun.*, 2005, 3661; (*c*) M. Kuil, P. E. Goudriaan, A. W. Kleij, D. M. Tooke, A. L. Spek, P. W. N. M. van Leeuwen and J. N. H. Reek, *Dalton Trans.*, 2007, 2311; (*d*) J. Flapper and J. N. H. Reek, *Angew. Chem., Int. Ed.*, 2007, **46**, 8590.

7 (*a*) A. J. Sandee, A. M. van der Burg and J. N. H. Reek, *Chem. Commun.*, 2007, 864; (*b*) J. M. Takacs, D. S. Reddy, S. A. Moteki, D. Wu and H. Palencia, *J. Am. Chem. Soc.*, 2004, **126**, 4494; (*c*) N. C. Gianneschi, P. A. Bertin, S. T. Nguyen, C. A. Mirkin, L. N. Zakharov and A. L. Rheingold, *J. Am. Chem. Soc.*, 2003, **125**, 10508; (*d*) C. J. Brown, G. M. Miller, M. W. Johnson, R. G. Bergman and K. N. Raymond, *J. Am. Chem. Soc.*, 2011, **133**, 11964; (*e*) C. J. Hastings, M. D. Pluth, R. G. Bergman and K. N. Raymond, *J. Am. Chem. Soc.*, 2010, **132**, 6938; (*f*) V. Bocokić, M. Lutz, A. L. Spek and J. N. H. Reek, *Dalton Trans.*, 2012, **41**, 3740.

8 For some early examples: (*a*) V. F. Slagt, P. W. N. M. van Leeuwen and J. N. H. Reek, *Angew. Chem., Int. Ed.*, 2003, **42**, 5619; (*b*) V. F. Slagt, J. N. H. Reek, P. C. J. Kamer and P. W. N. M. van Leeuwen, *Angew. Chem., Int. Ed.*, 2001, **40**, 4271.

9 A. D. Phillips, L. Gonsalvi, A. Romerosa, F. Vizza and M. Peruzzini, *Coord. Chem. Rev.*, 2004, **248**, 955.

10 (*a*) A. M. Castilla, S. Curreli, M. Martínez Belmonte, E. C. Escudero-Adán, J. Benet-Buchholz and A. W. Kleij, *Org. Lett.*, 2009, **11**, 5218; (*b*) E. C. Escudero-Adán, M. Martínez Belmonte, J. Benet-Buchholz and A. W. Kleij, *Org. Lett.*, 2010, **12**, 4592; (*c*) E. C. Escudero-Adán, M. Martínez Belmonte, E. Martin, G. Salassa, J. Benet-Buchholz and A. W. Kleij, *J. Org. Chem.*, 2011, **76**, 5404; (*d*) A. W. Kleij, *Eur. J. Inorg. Chem.*, 2009, 193; (*e*) A. W. Kleij, D. M. Tooke, M. Lutz, A. L. Spek and J. N. H. Reek, *Eur. J. Inorg. Chem.*, 2005, 4626.

11 S. J. Wezenberg, G. Salassa, E. C. Escudero-Adán, J. Benet-Buchholz and A. W. Kleij, *Angew. Chem., Int. Ed.*, 2011, **50**, 713.

12 A. W. Kleij, D. M. Tooke, M. Kuil, M. Lutz, A. L. Spek and J. N. H. Reek, *Chem.–Eur. J.*, 2005, **11**, 4743.

13 M. Martínez Belmonte, S. J. Wezenberg, R. M. Haak, D. Anselmo, E. C. Escudero-Adán, J. Benet-Buchholz and A. W. Kleij, *Dalton Trans.*, 2010, **39**, 4541.

14 For some examples: (*a*) A. L. Singer and D. A. Atwood, *Inorg. Chim. Acta*, 1998, **277**, 157; (*b*) S. J. Wezenberg, E. C. Escudero-Adán, J. Benet-Buchholz and A. W. Kleij, *Inorg. Chem.*, 2008, **47**, 2925.

15 SPECFIT/32, version 3.0.40, Spectra Software Associates, R. A. Binstead and A. D. Zuberbühler, 1993–2007; original publication; H. Gampp, M. Maeder, C. J. Meyer and A. D. Zuberbühler, *Talanta*, 1985, **32**, 95.

16 K. Chichak, U. Jacquemard and N. R. Branda, *Eur. J. Inorg. Chem.*, 2002, 357.

17 A. W. Kleij, M. Kuil, D. M. Tooke, A. L. Spek and J. N. H. Reek, *Inorg. Chem.*, 2005, **44**, 7696.

18 R. Bellini, S. H. Chikkali, G. Berthon-Gelloz and J. N. H. Reek, *Angew. Chem., Int. Ed.*, 2011, **50**, 7342.

19 O. Niyomura, T. Iwasawa, N. Sawada, M. Tokunaga, Y. Obora and Y. Tsuji, *Organometallics*, 2005, **24**, 3468.

20 A. J. Naaktgeboren, R. J. M. Nolte and W. J. Drenth, *J. Am. Chem. Soc.*, 1980, **102**, 3350.

21 See for instance: A. S. C. Chan and J. Halpern, *J. Am. Chem. Soc.*, 1980, **102**, 838.

22 See for instance: C.-W. Huang, K. Y. Chiu and S.-H. Cheng, *Dalton Trans.*, 2005, 2417.

23 G. M. Sheldrick, *SHELXTL Crystallographic System, version 6.10*, Bruker AXS, Inc., Madison, Wisconsin, 2000.

24 M. C. Burla, R. Caliandro, M. Camalli, B. Carrozzini, G. L. Cascarano, C. Giacovazzo, M. Mallamo, A. Mazzone, G. Polidori and R. Spagna, *J. Appl. Crystallogr.*, 2012, **45**, 357.

25 SQUEEZE: P. van der Sluis and A. L. Spek, *Acta Crystallogr., Sect. A: Fundam. Crystallogr.*, 1990, **46**, 194.

26 TWINABS Version 2008/4 Bruker AXS; R. Blessing, *Acta Crystallogr., Sect. A: Fundam. Crystallogr.*, 1995, **51**, 33.